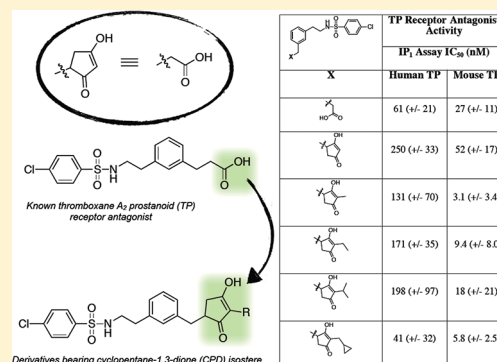


Cyclopentane-1,3-dione: A Novel Isostere for the Carboxylic Acid Functional Group. Application to the Design of Potent Thromboxane (A<sub>2</sub>) Receptor AntagonistsCarlo Ballatore,<sup>\*,†,‡</sup> James H. Soper,<sup>‡</sup> Francesco Piscitelli,<sup>†</sup> Michael James,<sup>‡</sup> Longchuan Huang,<sup>†</sup> Onur Atasoylu,<sup>†</sup> Donna M. Huryn,<sup>†</sup> John Q. Trojanowski,<sup>‡</sup> Virginia M.-Y. Lee,<sup>‡</sup> Kurt R. Brunden,<sup>‡</sup> and Amos B. Smith, III<sup>†</sup><sup>†</sup>Department of Chemistry, School of Arts and Sciences, University of Pennsylvania, 231 South 34th Street, Philadelphia, Pennsylvania 19104-6323, United States<sup>‡</sup>Center for Neurodegenerative Diseases Research, Department of Pathology and Laboratory Medicine, Institute on Aging, University of Pennsylvania, 3600 Spruce Street, Philadelphia, Pennsylvania 19104-6323, United States

## Supporting Information

**ABSTRACT:** Cyclopentane-1,3-diones are known to exhibit  $pK_a$  values typically in the range of carboxylic acids. To explore the potential of the cyclopentane-1,3-dione unit as a carboxylic acid isostere, the physical–chemical properties of representative congeners were examined and compared with similar derivatives bearing carboxylic acid or tetrazole residues. These studies suggest that cyclopentane-1,3-diones may effectively substitute for the carboxylic acid functional group. To demonstrate the use of the cyclopentane-1,3-dione isostere in drug design, derivatives of a known thromboxane A<sub>2</sub> prostanoid (TP) receptor antagonist, 3-(3-(2-(4-chlorophenylsulfonamido)ethyl)phenyl)propanoic acid (**12**), were synthesized and evaluated in both functional and radioligand-binding assays. A series of mono- and disubstituted cyclopentane-1,3-dione derivatives (**41–45**) were identified that exhibit nanomolar  $IC_{50}$  and  $K_d$  values similar to **12**. Collectively, these studies demonstrate that the cyclopentane-1,3-dione moiety comprises a novel isostere of the carboxylic acid functional group. Given the combination of the relatively strong acidity, tunable lipophilicity, and versatility of the structure, the cyclopentane-1,3-dione moiety may constitute a valuable addition to the palette of carboxylic acid isosteres.



## INTRODUCTION

Replacement of a specific atom, or group of atoms, with surrogates that exhibit similar physicochemical properties comprises a strategy known as isosteric replacement, adopted broadly by the medicinal chemistry community to improve the properties of a wide variety of biologically active compounds, such as potency, selectivity, metabolic/chemical stability, and ADME-PK properties.<sup>1,2</sup> A typical example of such a strategy is the replacement of a carboxylic acid moiety with a surrogate structure. Indeed, the presence of a carboxylic acid residue in the structure of a drug or drug candidate is often responsible for significant drawbacks, including limited permeability, toxicity, and metabolic instability.<sup>2</sup> At the same time, however, the acidity of the carboxylic acid residue may be required for biological activity; this is often the case when the carboxylic acid group is directly involved in relatively strong ionic interactions with the biological target (e.g., salt bridge within the active site of an enzyme). Under such circumstances, replacement of the carboxylic acid moiety with a surrogate structure may be beneficial. The outcome of any isosteric replacement, however, cannot be readily predicted, and thus, multiple isosteres are typically

required for evaluation. Among the most commonly employed isosteres of the carboxylic acid group, 1*H*-tetrazoles and 3-hydroxycyclobutene-1,2-diones (Figure 1A) proved to be useful in a number of cases.<sup>2,3</sup> Surprisingly, however, cyclopentanepolyones have not been evaluated as carboxylic acid surrogates, although the acidic properties of such compounds have been known for more than 50 years.<sup>4</sup> For example, cyclopentane-1,3-dione (CPD) and the 2-methyl congener (**1** and **2**, Figure 1) have been reported to have  $pK_a$  values of 4.4 and 4.7, respectively.<sup>4</sup> Equally important, nuclear magnetic resonance (NMR),<sup>5</sup> infrared (IR) absorption,<sup>5</sup> and X-ray crystal structure<sup>6,7</sup> studies demonstrate that such compounds exist almost exclusively as fast exchanging enol–ketone tautomers (see Figure 1B), which, like carboxylic acids, can establish “head-to-tail” intermolecular hydrogen bonds. In light of these interesting properties, we reasoned that CPDs may hold considerable promise as non-classical isosteres of the carboxylic acid moiety.

Received: July 22, 2011

Published: August 24, 2011

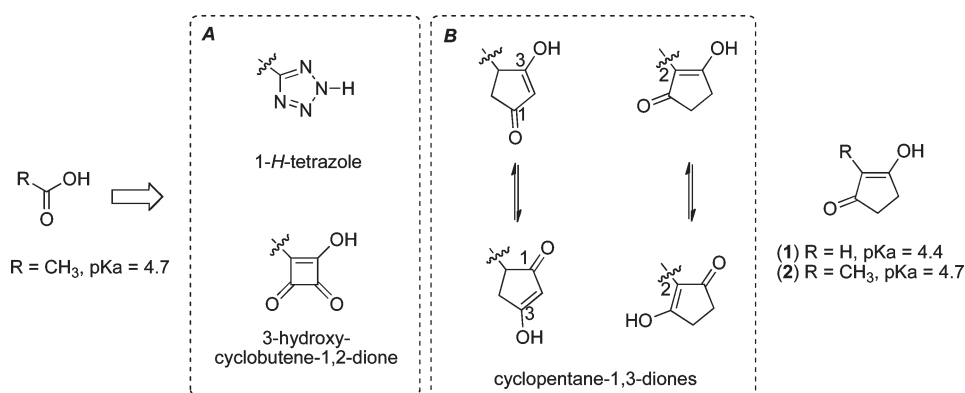


**Figure 1.** Selected examples of known (A) and proposed (B) isosteres of the carboxylic acid moiety.

To test this hypothesis, we designed, synthesized, and evaluated a focused set of model compounds to compare the physical chemical properties of similar structures bearing a carboxylic acid, tetrazole, or CPD residue. Electrospray ionization (ESI) mass spectrometry (MS), <sup>1</sup>H NMR, and computational techniques were employed to evaluate the ability of the congeners to form salts with benzamidine. To test the potential of CPD isosteres in drug design, we also designed, synthesized, and compared the biological properties of a series of CPD derivatives based on a representative thromboxane A<sub>2</sub> prostanoid (TP) receptor antagonist (**12**, Figure 2)<sup>8</sup> to the corresponding analogues bearing other carboxylic acid isosteres such as the tetrazole and amino squaric acid.

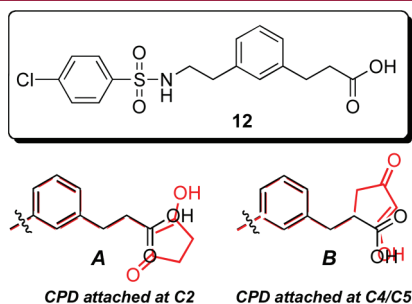


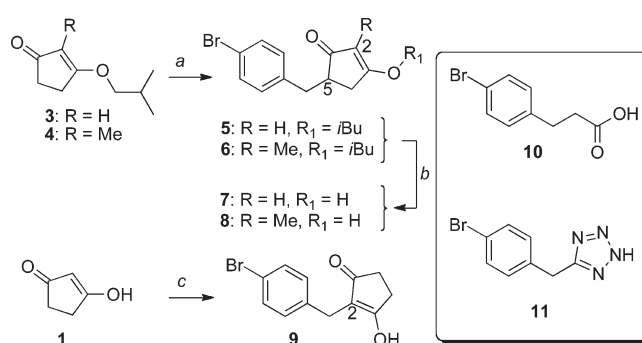
**Figure 2.** Structure of known TP-receptor antagonist **12** (top) and overlap of the carboxylic acid moiety of **12** with CPD derivatives attached at either C2 or C4/C5 (bottom, A or B, respectively).

## DESIGN AND SYNTHESIS OF MODEL COMPOUNDS

The CPD fragment presents two nonequivalent points of attachment (i.e., the C2 and one of the prochiral C4/C5 positions, Figure 1B) for analogue development. Thus, to evaluate the physical–chemical properties of CPDs relative to carboxylic acids and tetrazoles, representative model 2- and 5-monosubstituted (**9** and **7**, respectively, Scheme 1) and 2,5-disubstituted (**8**, Scheme 1) CPD derivatives were designed and synthesized. In each case, a 4-bromobenzyl moiety was used as a substituent to ensure appropriate solubility in organic solvents, a prerequisite to enable ESI-MS studies (vide infra).

Compounds **7** and **8** were prepared by reacting the appropriate lithiated 3-isobutoxycyclopent-2-enone (i.e., **3** or **4**) with 4-bromobenzyl bromide, under the reaction conditions developed by Koreeda and co-workers<sup>9</sup> to achieve regioselective

## Scheme 1<sup>a</sup>



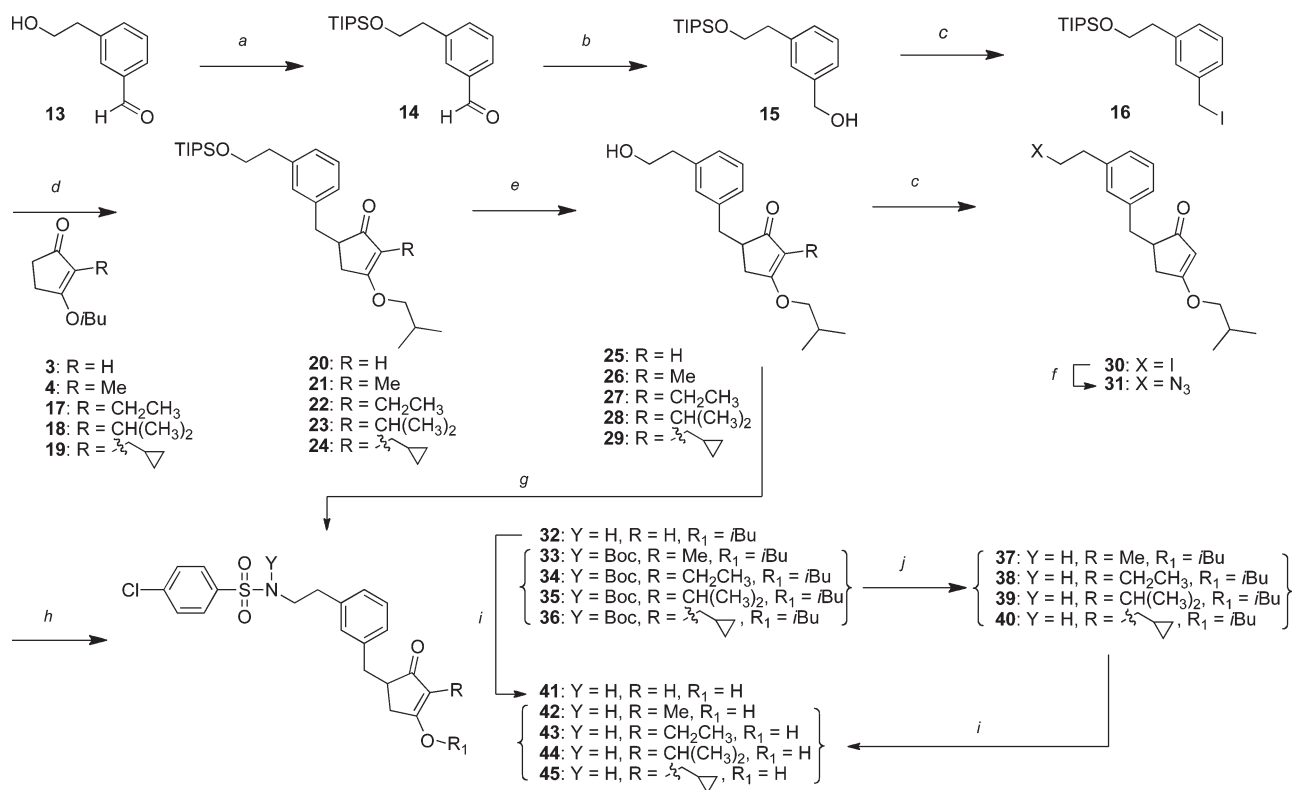
<sup>a</sup> Reagents and reaction conditions: (a) (i) lithium diisopropylamide, −78 °C; (ii) 4-bromobenzyl bromide, −78 °C to room temp over 1 h; (b) 2 N hydrochloric acid, acetone; (c) 4-bromobenzaldehyde, Hantzsch ester, L-proline, dichloromethane, room temp, 2 h.

alkylation at the C5 position, to obtain monoalkylated products **5** and **6** as racemic mixtures. Hydrolysis of the enol–ether under acidic conditions then furnished **7** and **8**. For the synthesis of the 2-substituted CPD **9**, we employed the reductive alkylation protocol reported by Ramachary and Kishor;<sup>10</sup> specifically, 4-bromobenzaldehyde was reacted with CPD in the presence of diethyl 1,4-dihydro-2,6-dimethyl-3,5-pyridinedicarboxylate (Hantzsch ester) to furnish **9**. Construction of tetrazole **11** was achieved as previously reported,<sup>11</sup> while the 4-bromophenylpropionic acid **10** was purchased.

## DESIGN AND SYNTHESIS OF CPD-CONTAINING TP-RECEPTOR ANTAGONISTS

With respect to TP-receptor antagonist design, depending on the point of attachment on the CPD moiety and the length of the aliphatic spacer, two alternative structures were envisioned, which exhibit a promising degree of overlap with the carboxylic acid moiety of the parent compound **12** (Figure 2). We therefore synthesized a series of both 2- and 5-substituted CPDs, as well as different 2,5-disubstituted CPD derivatives (Scheme 2). Tetrazole and amino squarate derivatives of **12** (respectively **61** and **62**, Table 2) were also constructed for comparison.

The synthesis of the 5-substituted CPD derivatives **41** and 2,5-disubstituted congeners **42–45** (Scheme 2) employed similar strategies as employed for **7** and **8**. In all cases, alkylation of the

Scheme 2<sup>a</sup>

<sup>a</sup> Reagents and reaction conditions: (a) (*i*-Pr)<sub>3</sub>Si-Cl, imidazole, *N,N*-dimethylformamide, 0 °C, 3 h; (b) NaBH<sub>4</sub>, H<sub>2</sub>O, tetrahydrofuran, 70 °C, 2 h; (c) PPh<sub>3</sub>, I<sub>2</sub>, imidazole, Et<sub>2</sub>O, acetonitrile, 0 °C, 2 h; (d) appropriate isobutyl-protected cyclopentane-1,3-dione, lithium diisopropylamide, tetrahydrofuran, from -78 °C to room temp; (e) tetra-*n*-butylammonium fluoride, tetrahydrofuran, 0 °C, 3 h; (f) NaN<sub>3</sub>, *N,N*-dimethylformamide, 50 °C, 45 min; (g) PPh<sub>3</sub>, diethyl azodicarboxylate, *tert*-butyl (4-chlorophenyl)sulfonylcarbamate, tetrahydrofuran, room temp, 4 h; (h) (i) H<sub>2</sub>, Pd-C, methanol, room temp, 16 h, (ii) 4-chlorobenzenesulfonyl chloride, 2 N NaOH, 0 °C, 3 h; (i) 2 N HCl, acetone, room temp, 6–12 h; (j) 2,2,2-trifluoroacetic acid, dichloromethane, room temp, 2–5 h.

CPD was achieved by reacting the appropriate lithiated 3-isobutoxycyclopent-2-enone<sup>9</sup> (i.e., 3, 4, 17–19) with benzyl iodide 16, obtained in three steps from aldehyde 13, to furnish 20–24 (Scheme 2). Removal of the silyl-protecting group then furnished alcohols 25–29. For installation of the phenylsulfonamide moiety, we initially employed a reaction sequence consisting of (a) conversion of alcohol 25 to the corresponding alkyl iodide 30, (b) displacement of the iodide with sodium azide (31), and (c) reduction of the latter to the corresponding amine, followed by in situ sulfonylation of the amine with 4-chlorobenzenesulfonyl chloride to yield 32 (Scheme 2). Similar overall transformations could be achieved in comparatively fewer steps and in higher overall yield by treating alcohols 26–29 with *N*-Boc-protected phenylsulfonamide under Mitsunobu conditions<sup>12</sup> to furnish 33–36. Finally, treatment of 32 with 2 N hydrochloric acid in acetone provided the desired compound 41, whereas 33–36 were subjected to stepwise deprotection of the Boc carbamate and enol-ether, respectively, to furnish 37–40 and 42–45 (Scheme 2).

Construction of the 2-substituted CPD derivatives, 50 and 59 (Scheme 3), began with aldehydes 14 and 54, respectively. Silyl-protected aldehyde 54 was obtained from diacid 51 via lithium aluminum hydride reduction, followed in turn by protection as silyl ether of one of the hydroxyl moieties (53) and pyridinium dichlorochromate mediated oxidation of the free hydroxyl. The

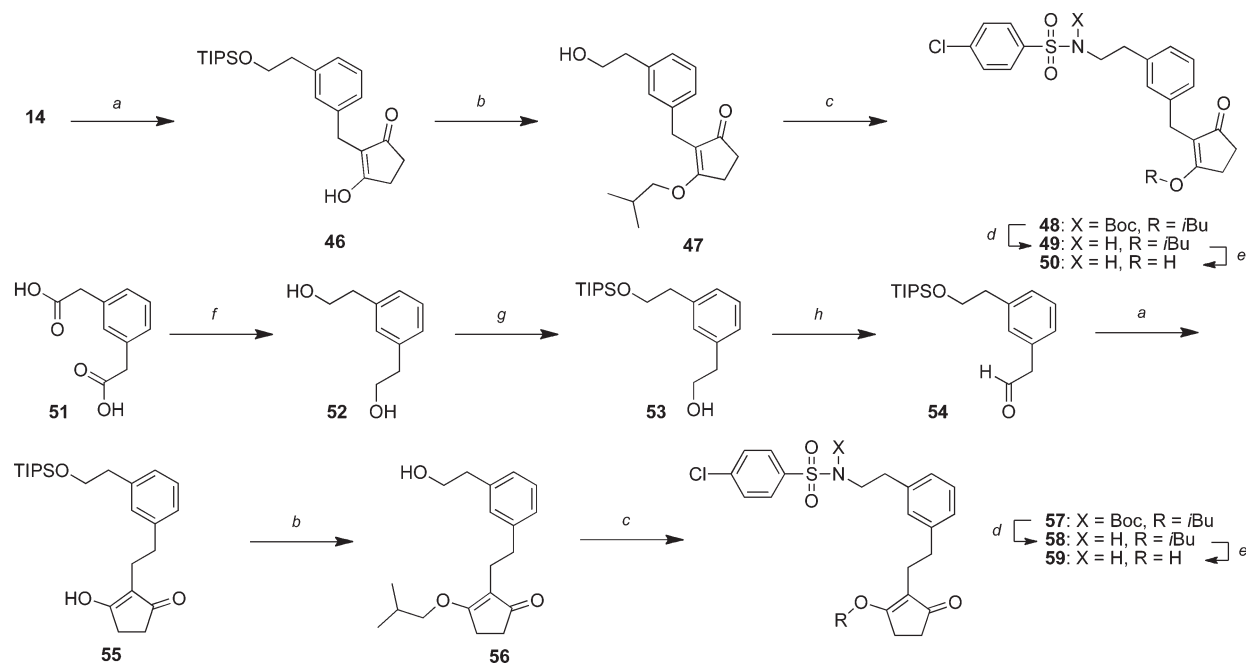
aldehydes (14, 54) were then reacted with CPD under the previously described reductive alkylation conditions<sup>10</sup> to furnish the 2-alkylated CPD derivatives 46 and 55. These intermediates were then directly converted to alcohols 47 and 56 by treatment with isobutanol/benzene in the presence of a catalytic amount of *p*-toluenesulfonic acid at reflux. Installation of the *N*-Boc-protected 4-chlorophenylsulfonamide moiety via Mitsunobu reaction<sup>12</sup> and removal of Boc and isobutyl ether protecting groups then furnished the desired 2-substituted CPD derivatives 50 and 59.

Syntheses of carboxylic acid 12 (Figure 2), the corresponding alcohol 60, tetrazole 61, and amino squaric acid 62 (Table 1) are detailed in the Supporting Information.

## PHYSICAL-CHEMICAL PROPERTY EVALUATION

The lipophilicity and/or acidity of compounds 1, 2, 7–11 was determined experimentally, followed by an examination of their ability to form salts with benzamidine, the latter investigated by ESI-MS and NMR. Finally, computational studies were carried out to estimate the structure and stability of the complexes of CPD derivatives with benzamidine.

**Determination of pK<sub>a</sub> and log P.** pK<sub>a</sub> values of compounds 1, 2, 7–11, as well as the log P and log D<sub>pH 7.4</sub> values of compounds 7–11, were determined experimentally by Sirius Analytical

Scheme 3<sup>a</sup>

<sup>a</sup> Reagents and reaction conditions: (a) CPD (**1**), Hantzsch ester, L-proline, dichloromethane, room temp, 12 h; (b) *p*-toluenesulfonic acid (cat.), isobutanol/benzene, reflux, 16 h; (c) *tert*-butyl (4-chlorophenyl)sulfonylcarbamate, PPh<sub>3</sub>, diethyl azodicarboxylate, tetrahydrofuran, room temp, 4 h; (d) 2,2,2-trifluoroacetic acid, dichloromethane, room temp, 2 h; (e) 2 N hydrochloric acid, acetone, room temp, 12 h; (f) LiAlH<sub>4</sub>, diethyl ether, -78 °C, 3 h; (g) (*i*-Pr)<sub>3</sub>Si-Cl, imidazole, *N,N*-dimethylformamide, 0 °C, 3 h; (h) pyridinium chlorochromate, dichloromethane, room temp, 2 h.

(UK) via UV-metric or potentiometric (pH-metric) methods. The results are summarized in Table 1 (see Supporting Information for full reports).

**Evaluation of the Ability of Model CPD Derivatives to Form Salts with Benzamidine.** The structure and stability of the amidine complexes with carboxylate and tetrazolate anions have been investigated with a combination of ESI-MS and NMR techniques,<sup>13,14</sup> suggesting that this experimental model could be useful to evaluate and compare carboxylic acid isosteres. Thus, we employed similar strategies to evaluate the ability of CPDs **7–9** to form salts with amidines. For ESI-MS studies, a 10 μM solution of each test compound in acetonitrile was mixed with an equal volume of a 10 μM solution of benzamidine in acetonitrile. The solubility of **7–11** in acetonitrile had been predetermined, and each of the compounds was found to be fully soluble at 10 μM (see Supporting Information). After a 5 min incubation period, the resulting mixtures were analyzed by ESI-MS to detect

the mass of the [CPD·benzamidine] complex. As illustrated in Figure 3, in all cases the test compound·benzamidine ion<sup>+</sup> was readily detectable by ESI-MS.

Competition-binding studies were conducted by comparing the intensity of the signal corresponding to the [8·benzamidine] complex with and without coaddition of a competing acid/acid surrogate (i.e., **7**, **9–11**; see Figure 4). In these experiments, benzamidine, compound **8**, and the competing acid/acid surrogate were mixed in a 1:1:1 ratio in acetonitrile and after a 5 min incubation time, the mixtures were analyzed by ESI-MS to monitor for the presence of the [8·benzamidine] complex. The relative intensity of the [8·benzamidine] complex in the presence or absence of competing acid/acid surrogate provided qualitative information on the binding affinity of CPD derivatives for amidines, compared to acid **10** or tetrazole **11** (Figure 4). As shown in Figure 4, co-incubation of equimolar amounts of benzamidine, **8**, and **9** resulted in a ~50% reduction in the peak intensity assigned to the [8·benzamidine] complex, while analogous co-incubations of benzamidine and **8** with **7**, **10**, or **11** resulted in a comparatively smaller reduction (i.e., <50%) of the [8·benzamidine] signal. Thus, under the experimental conditions employed in the competition studies, all CPD derivatives appeared to have greater affinity for benzamidine than either the corresponding carboxylic acid (**10**) or tetrazole (**11**) compound (Figure 4).

The interaction of the CPD–benzamidine complex was also investigated by <sup>1</sup>H NMR. The observed upfield shift of the signal corresponding to the proton in position 2 of CPD **1** at different molar ratios with benzamidine was used to conduct Job plot analysis (see Supporting Information).<sup>15</sup> On the basis of such an analysis, the minimum of the plot corresponds to the

Table 1. pK<sub>a</sub>, log P, and log D<sub>pH 7.4</sub><sup>a</sup>

compd	pK <sub>a</sub>	log P	log D <sub>pH 7.4</sub>
<b>1</b>	4.20 ± 0.01 (4.4) <sup>b</sup>	ND <sup>c</sup>	ND <sup>c</sup>
<b>2</b>	4.47 ± 0.01 (4.7) <sup>b</sup>	ND <sup>c</sup>	ND <sup>c</sup>
<b>7</b>	3.96 ± 0.01	3.02 ± 0.01	-0.42
<b>8</b>	4.24 ± 0.01	3.28 ± 0.01	0.11
<b>9</b>	4.20 ± 0.02	3.01 ± 0.01	-0.19
<b>10</b>	4.33 ± 0.01	3.00 ± 0.01	0.01
<b>11</b>	4.62 ± 0.01	2.21 ± 0.01	-0.42

<sup>a</sup> All determinations were carried out via UV-metric or potentiometric (pH-metric) method. <sup>b</sup> Literature value. <sup>c</sup> Not determined.

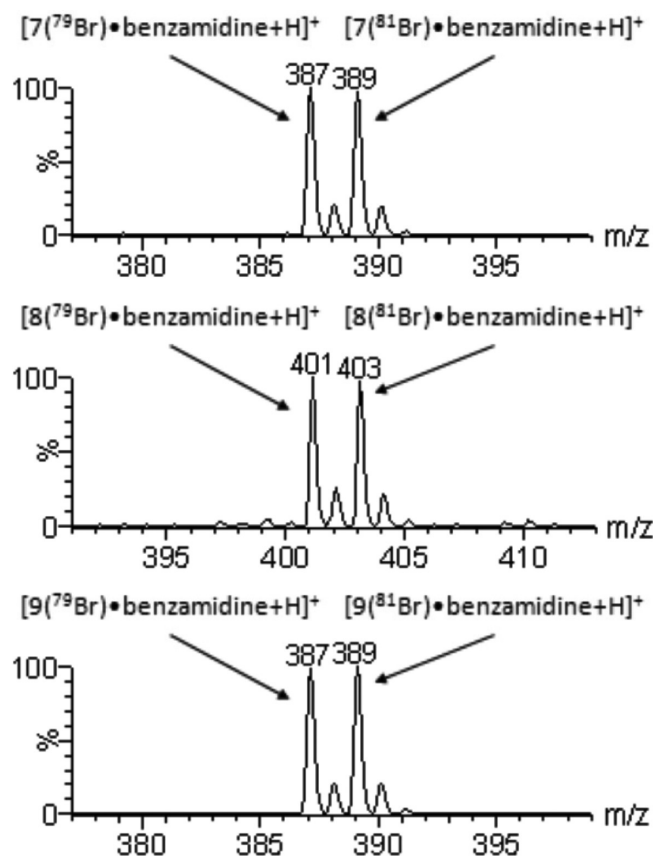


Figure 3. [CPD·benzamidinium]<sup>+</sup> complexes detected by ESI-MS.

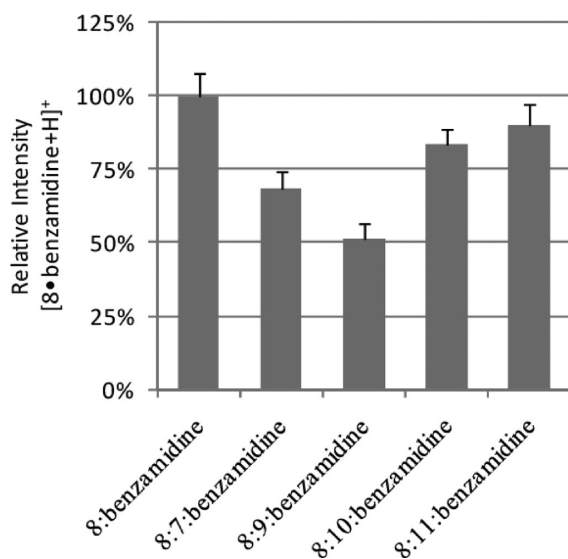


Figure 4. Relative intensity of the [8·benzamidinium]<sup>+</sup> signal in a 1:1 mixture of 8 and benzamidinium (100%) or in 1:1:1 mixtures of 8, benzamidinium, and competing acid/acid surrogate (i.e., 7, 9–11).

stoichiometry of the CPD–benzamidinium interaction. These studies confirmed that CPD forms a 1:1 complex with benzamidinium (Figure 5).

**Computational Studies.** CPDs possess two tautomeric forms that can potentially generate different salt bridge geometries.

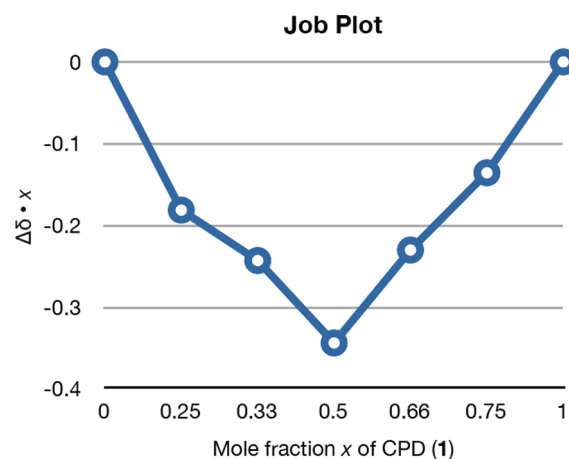
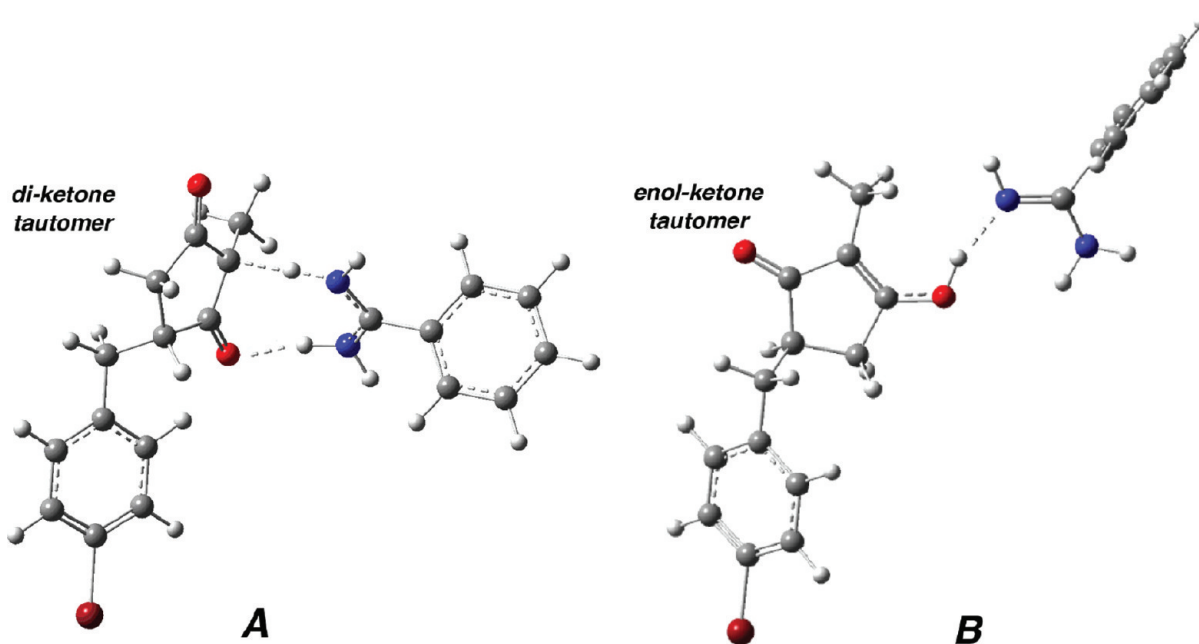


Figure 5. <sup>1</sup>H NMR Job plot analysis of [1·benzamidinium] complex showing 1:1 stoichiometry. The plot is derived from the chemical shift of the C2-H of 1 at different molar ratios with benzamidinium. The total concentration is kept constant (i.e., 0.125 M) in each experiment. The mole fraction  $x$  is defined as  $[1]/([1] + [\text{benzamidinium}])$ ;  $\Delta\delta = \delta_{\text{complex}} - \delta_{\text{free}}$ .

Initially, quantum mechanical (QM) calculations were performed both to explore the ground state geometries and to define the energy differences of the two tautomeric forms of a representative CPD (i.e., 7 and 8). These studies revealed that regardless of solvent medium (i.e., no solvent/vacuum, water, or chloroform), the enol–ketone tautomer is comparatively more stable than the diketone tautomer (e.g., for 8 the energy difference is 0.91 kcal/mol, B3LYP 6-31G+(d,p) in the gas phase, and on average 0.74 kcal/mol in water and chloroform; see Supporting Information). Next, the geometry and stability of [8·benzamidinium] complexes were investigated. Optimization of possible salt geometries revealed two possible scenarios (A and B), originating from the initial tautomers (i.e., diketone and enol–ketone): (a) a bicoordinated “stacked” geometry (Figure 6A) characterized by two intermolecular interactions between the diketone tautomer and the amidine moiety; (b) a monocoordinated “linear” geometry, wherein a single interaction between the amidine nitrogen and the enolate oxygen is observed (Figure 6B). Quantum mechanical calculations (gas phase) and with a water solvation model suggest that the latter salt bridge geometry (Figure 6B) is more stable than the former. Disruption of the  $\pi$  system in the geometry in Figure 6A is believed to be responsible for the energy difference. Calculated energies for the monocoordinated CPD salt (Figure 6B) were found to be similar to those corresponding to the bicoordinated salt bridges of carboxylic acids with amidine bases (see Supporting Information).

## ■ BIOLOGICAL EVALUATION

To evaluate whether CPD isosteres could mimic the activity of biologically active compounds, CPD analogues 41–45 and 59 were evaluated for their ability to act as antagonists of the human and mouse TP-receptor by a functional inositol monophosphate (IP<sub>1</sub>) assay that measures receptor activation. The activity of test compounds was compared with known antagonist 12,<sup>8</sup> as well as with tetrazole 61 and amino squaric acid 62. Analogues 37–39 and 50 were also examined for comparison. Briefly, the IP<sub>1</sub> assay depends on a homogeneous time-resolved fluorescence method that permits the measurement of IP<sub>1</sub>, which is a stable metabolite of the intercellular signal transduction molecule, inositol triphosphate



**Figure 6.** Calculated bicoordinated “stacked” (A) and monocoordinated “linear” (B) geometries of the [8·benzamide] complex in gas phase.

(IP<sub>3</sub>). Activation of the TP-receptor is known to result in increased release of IP<sub>3</sub>;<sup>16</sup> thus, an antagonist to this receptor will inhibit agonist-induced increase of IP<sub>1</sub> in QBI293 cells that have been stably transfected with the human or mouse TP receptor. As illustrated in Table 2, a range of CPD analogues were evaluated and derivatives 42–45 exhibited activity comparable to that of the known antagonist 12 as well as those of the tetrazole and amino squarate derivatives (61 and 62, respectively).

Finally, the binding affinity of a representative subset of active and inactive compounds against the human and mouse TP-receptor was evaluated via radioligand scintillation proximity assay. In this assay, membrane preparations from cells expressing the human or mouse TP receptor associate with scintillant beads that emit measurable photons upon binding of the radiolabeled TP antagonist, [<sup>3</sup>H]SQ 29548, to receptors within the membrane. Thus, a ligand that competes for binding of the radiolabeled compound to the TP-receptor will cause a concentration-dependent decrease in signal that can be quantified to yield a binding constant for the competitive molecule.<sup>17</sup> Consistent with the functional assay results, these radioligand binding studies reveal that CPD derivatives 41 and 42 exhibit binding affinity values that are comparable to that of the known antagonist 12, as well as those of the tetrazole (61) and the amino squarate (62) derivatives (Table 3).

## ■ DOCKING STUDIES

A TP-receptor model was developed via homology modeling as previously described.<sup>18</sup> Docking studies were then carried out using the Autodock software package, initially employing the natural ligand thromboxane A<sub>2</sub> (TXA<sub>2</sub>). Since previous reports suggest that Arg-295 and Ser-201 residues in the intracellular region are important constituents of the binding pocket within the TP-receptor,<sup>19</sup> docking of TXA<sub>2</sub> was conducted by setting a salt bridge between the carboxylic acid residue of TXA<sub>2</sub> and the side chain of Arg-295 as a constraint. In agreement with previous docking studies by Yamamoto and co-workers,<sup>20</sup> our studies indicate that the polycarbon side chain of TXA<sub>2</sub> extends into the

intracellular hydrophobic segment between the III, V, and VI helices, with a favorable hydrogen bond to the Ser-201 residue (Figure 7A). Next, the binding modes of compound 12, and of a representative CPD derivative (42), were evaluated and compared (Figure 7B and Figure 7C, respectively). As shown in Figure 7B,C and in Figure 8, compounds 12 and 42 were found to share similar hydrophobic interactions between the central phenyl ring and the pocket formed by Leu-261, Leu-294, Ala-297, and Met-112, as well as between the phenylsulfonamide moiety and the pocket between helices III and IV (Trp-258 and Gly-116, see Figure 8). Interestingly, while the carboxylic acid moiety of 12 interacted with Arg-295 via the expected bicoordinated salt bridge, the corresponding CPD isostere in 42 was found to establish a monocoordinated salt bridge with the guanidinium moiety of Arg-295 as well as a hydrogen bond with the backbone nitrogen of Thr-298 (Figure 8). Equally interesting, the 2-position of the CPD fragment appears to be directed through the groove of helix VII, suggesting that an increase in steric hindrance at this position may be well tolerated. This observation is consistent with functional and receptor binding data (cf., Tables 2 and 3).

## ■ DISCUSSION

Although CPDs share important similarities with the carboxylic acid moiety, including comparable pK<sub>a</sub> values and the ability to establish H-bonds, there are no reports of this isostere employed as a surrogate of the carboxylic acid moiety in drug design. To evaluate CPDs as potential carboxylic acid isosteres, we compared the properties of representative mono- and disubstituted CPD analogues with similar compounds bearing carboxylic acid or tetrazole moieties. These studies confirmed the intrinsic acidity of the CPD fragment and revealed that compounds 7–9, depending on the substitution pattern, can be somewhat more acidic than the corresponding carboxylic acid and tetrazole counterparts. Furthermore, the lipophilicity of these compounds is also either equal or higher than acid 10 and tetrazole 11 (Table 1). Importantly, the ability of CPD

Table 2. TP-Receptor Antagonist Activity of Test Compounds

Cpd#	X	TP Receptor Antagonist Activity IP <sub>1</sub> Assay IC <sub>50</sub> (nM)	
		Human TP	Mouse TP
12		61 (+/- 21)	27 (+/- 11)
60		15117 (+/- 7994)	1627 (+/- 721)
61		64 (+/- 41)	8.0 (+/- 6)
62		377 (+/- 203)	91 (+/- 33)
50		>10,000	>10,000
59		>10,000	1229 (+/- 462)
41		250 (+/- 33)	52 (+/- 17)
42		131 (+/- 70)	3.1 (+/- 3.4)
37		>10,000	1786 (+/- 1212)
43		171 (+/- 35)	9.4 (+/- 8.0)
38		3801 (+/- 443)	463 (+/- 250)
44		198 (+/- 97)	18 (+/- 21)
39		5303 (+/- 1078)	259 (+/- 90)
45		41 (+/- 32)	5.8 (+/- 2.5)
40		21853 (+/- 2151)	2524 (+/- 233)

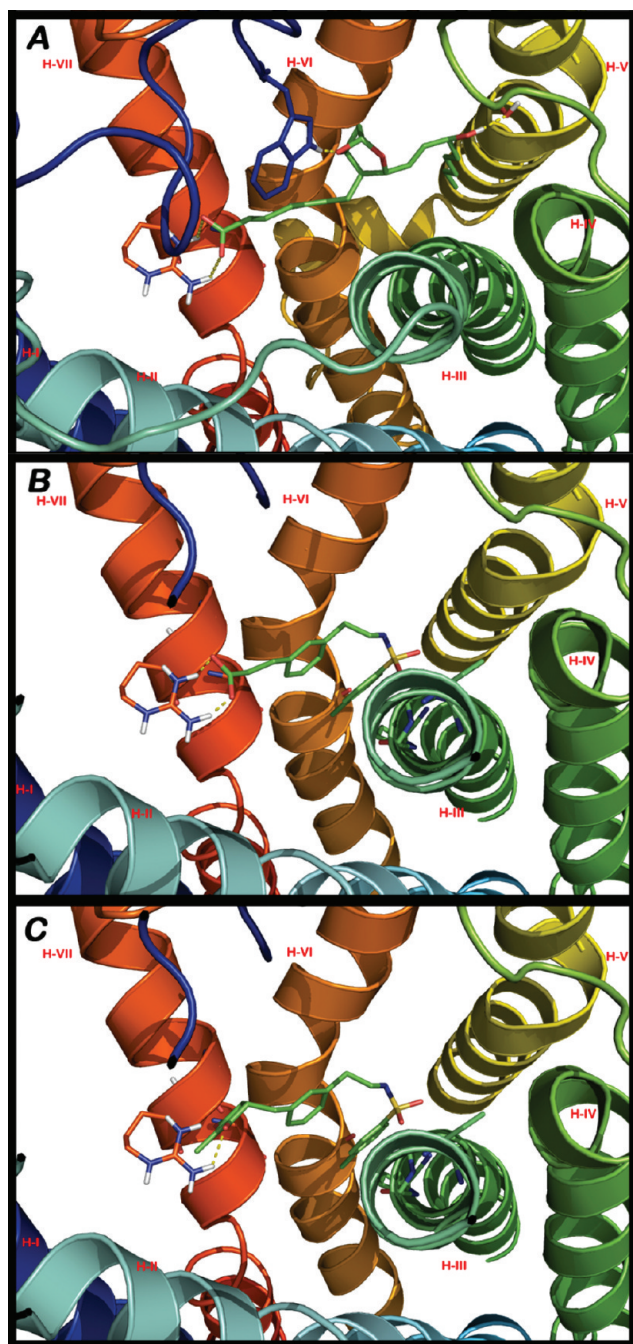
derivatives 7–9 to form complexes with benzamidine was demonstrated by ESI-MS and NMR. Of particular note, our studies suggest that CPDs can reversibly form 1:1 complexes with benzamidine regardless of the substitution pattern (cf., Figures 3 and 5). Computational studies indicated that the most likely salt bridge geometry involves monocoordinated structures between the amidine nitrogen and the enolate oxygen of the CPD. Although our studies focused exclusively on the CPD–benzamidine complexes, similar salt geometries may also exist between CPDs and other amines, including the amino groups on lysine and histidine side chains. Interestingly, results from competition-binding studies indicate that, under the experimental conditions, the CPD–benzamidine complex may be more stable than the corresponding tetrazolate–benzamidine or carboxylate–benzamidine complexes (Figure 4). These results do not appear to correlate exactly with either the  $pK_a$  values or

Table 3. TP-Receptor Binding Affinity of Selected Compounds, Determined by Radioligand-Binding Assay

Cpd#	X	TP Receptor Binding Scintillation Proximity Assay K <sub>d</sub> (nM)	
		Human TP	Mouse TP
12		141 (+/- 31)	26 (+/- 9.6)
60		>10,000	>10,000
61		331 (+/- 109)	19 (+/- 9.0)
62		359 (+/- 60)	17 (+/- 7.5)
50		11400 (+/- 3960)	1196 (+/- 1334)
41		203 (+/- 87)	11 (+/- 9.5)
42		328 (+/- 87)	26 (+/- 5.7)

calculated salt bridge formation energies; however, the lack of correlation observed may be due to the experimental conditions employed in the ESI-MS studies, particularly the fact that these experiments are performed in organic solvent. Taken together, these results strongly suggested that the CPD fragment holds great promise as an effective surrogate for the carboxylic acid moiety.

To verify this hypothesis in the context of a biologically active system, analogues of the known TP-receptor antagonist **12**<sup>8</sup> were designed by replacing the carboxylic acid moiety of this compound with a CPD fragment linked at either the C2 or C5 position (Figure 2). The TP-receptor is an important G-protein-coupled receptor (GPCR) implicated in several pathophysiological processes, such as vasoconstriction, aggregation of platelets,<sup>21</sup> and more recently, Alzheimer's disease.<sup>22</sup> A number of TP-receptor antagonists have been reported, and many of these, like **12**, comprise an aromatic ring connected to both a phenylsulfonamide and a carboxylic acid moiety via intervening aliphatic spacers, typically of two to three carbons in length.<sup>21</sup> Previous studies suggest that the carboxylic acid moiety of TP-receptor antagonists are involved in the formation of a salt bridge with Arg-295 of the receptor.<sup>20</sup> Thus, the presence of a carboxylic acid moiety may be a general prerequisite for receptor binding and activity. This requirement is clearly the case for compound **12**, as highlighted by the dramatic loss in activity in both the functional and radioligand-binding assays observed when the corresponding alcohol derivative **60** is employed (Tables 2 and 3). Conversely, replacement of the carboxylic acid moiety with either tetrazole (**61**) or squaric acid (**62**) led to derivatives with activity and binding affinity generally comparable to **12**. Among the CPD derivatives, interesting differences emerged depending on where the CPD moiety is attached (i.e., C2 or C5). While C2 substituted derivatives **50** and **59** were essentially devoid of any activity in the functional assay, all C5 substituted compounds (**41**–**45**) exhibited IC<sub>50</sub> values in the same range of carboxylic acid **12** (Table 2). These observations were confirmed by radioligand-binding data (Table 3), demonstrating that representative examples of C2 and C5 linked CPD derivatives exhibited



**Figure 7.** Docking of thromboxane A<sub>2</sub> (A), 12 (B), and 42 (C) to the TP-receptor.

drastically different binding affinities. Given that ESI-MS studies with model compounds 7–9 did not reveal significant differences between the C2 and C5 linked CPD congeners in their ability to generate complexes with benzamidine, the results from the functional assay suggest that the position and/or orientation of the enol–ketone moiety may prove critical in the relatively confined environment of the receptor. Also of note, the steric hindrance of the C2 substituents of 41–45 did not appear to impact the activity of the analogues, suggesting that effective electrostatic interactions with the TP-receptor may take place if the CPD moiety is linked at C5, even in the presence of relatively large substituents linked at C2. Consistent with these results, docking studies revealed that the

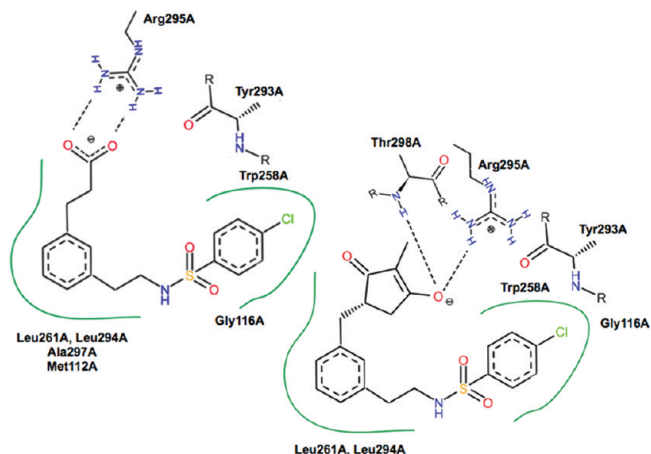


**Figure 8.** Schematic representation of key interactions of 12 and 42 with TP-receptor.

2-position of the CPD can be adjacent to the groove of helix VII of the TP-receptor, indicating that steric hindrance at the C2 would be relatively well tolerated. This characteristic may be exploited to design analogues with increased complementarity with the receptor and/or to modify the physical–chemical properties (e.g., lipophilicity) of the compound.

## CONCLUSIONS

Collectively, the studies presented here demonstrate that the CPD fragment comprises a viable new surrogate for the carboxylic acid moiety with potential applications in drug design. In addition to the significant intrinsic acidity and the ability to form salt bridges, our results demonstrate that the CPD moiety may permit substantial structural differentiation of the acidic residue. This characteristic may be particularly desirable when attempting to modulate drug–target/off-target interactions and/or physical–chemical properties of biologically active compounds. As a result, the CPD would appear to be a valuable addition to the existing palette of carboxylic acid isosteres.

## EXPERIMENTAL SECTION

**Materials and Methods.** All solvents were reagent grade. All reagents were purchased from Aldrich or Acros and used as received. Thin layer chromatography (TLC) was performed with 0.25 mm E. Merck precoated silica gel plates. Flash chromatography was performed with silica gel 60 (particle size 0.040–0.062 mm) supplied by Silicycle and Sorbent Technologies. Spots were detected by viewing under a UV light. Yields refer to chromatographically and spectroscopically pure compounds. Infrared spectra were recorded on a Jasco Model FT/IR-480 Plus spectrometer. All melting points were obtained on a Thomas-Hoover apparatus. Proton (<sup>1</sup>H) and carbon (<sup>13</sup>C) NMR spectra were recorded on a Bruker AMX-500 spectrometer. Chemical shifts were reported relative to solvents (CDCl<sub>3</sub> 7.27 ppm; CD<sub>3</sub>OD 3.35 ppm; DMSO-*d*<sub>6</sub> 2.5 ppm, acetone-*d*<sub>6</sub> 2.05 ppm). As previously observed,<sup>10</sup> CPDs are mixtures of rapidly interconverting tautomers that can complicate the interpretation of <sup>13</sup>C NMR spectra. High-resolution mass spectra were measured at the University of Pennsylvania Mass Spectrometry Service on either a VG Micromass 70/70H or VG ZAB-E spectrometer. Single-crystal X-ray structure determinations were performed at the University of Pennsylvania with an Enraf Nonius CAD-4 automated diffractometer. Analytical reversed-phased (Sunfire C18; 4.6 mm × 50 mm, 5 mL) high-performance liquid chromatography (HPLC) was performed with a













in acetonitrile were vortexed at room temperature for 5 min and then infused using the detector's syringe pump at 30  $\mu\text{L}/\text{min}$ . Mass spectra were acquired in positive ion mode with a 0.5 s scan rate over 30 s. Scans 1–50 were combined and analyzed.

**CPD–Benzamidine Relative Affinity by Competition.** Compound **8** and benzamidine were mixed with a competing acid at equimolar amounts (10  $\mu\text{M}/10 \mu\text{M}/10 \mu\text{M}$ ) in acetonitrile. Mixtures were vortexed at room temperature for 10 min and then infused into the mass spectrometer at 30  $\mu\text{L}/\text{min}$ . After stabilization of the infusion flow, mass spectra were acquired in positive ion mode with a 0.2 s scan rate over 30 s. Scans 1–100 were combined, and the intensity of the 8–benzamidine salt ion,  $[8(^{79}\text{Br})\cdot\text{benzamidine} + \text{H}]^+$  ( $m/z$  401), was recorded. Affinities between acids and the benzamidine base were determined relative to **8** as the average ( $N = 3$ ) reduction of intensity of the 8–benzamidine salt ion in the presence of a competing acid.

**IP<sub>1</sub> Functional Assay.** The activity of the TP-receptor was measured by quantifying cellular levels of the IP<sub>3</sub> metabolite, IP<sub>1</sub>, using a homogeneous time-resolved fluorescence (HTRF) assay kit (IP-One Tb, Cisbio, Bedford, MA, U.S.). QBI-HEK 293A cells that were stably transfected with human or mouse TP receptor cDNA were plated into 384-well plates at 10 000 cells/well in DMEM containing 4.5 g/L glucose, 10% fetal bovine serum, L-glutamine, and penicillin/streptomycin. The cells were incubated for 16 h at 37 °C with 5% CO<sub>2</sub>, after which culture medium was removed and the cells were then incubated for 15 min at 37 °C with 5% CO<sub>2</sub> in 10 mM Hepes, 1 mM CaCl<sub>2</sub>, 0.4 mM MgCl<sub>2</sub>, 4.2 mM KCl, 146 mM NaCl, 5.5 mM glucose, 50 mM LiCl, pH 7.4, containing varying concentrations of test antagonist. The TP receptor agonist, I-BOP ([15-(1 $\alpha$ ,2 $\beta$ (5Z),3 $\alpha$ -(1E,3S),4 $\alpha$ )]-7-[3-hydroxy-4-(*p*-iodophenoxy)-1-butenyl-7-oxabicycloheptenoic acid]), was added at 1.6 nM and incubated for 1 h at 37 °C with 5% CO<sub>2</sub>. Tb-labeled anti-IP<sub>1</sub> cryptate and D2-labeled IP<sub>1</sub> were subsequently added in lysis buffer and incubated for 1 h at 25 °C according to the manufacturer's instructions. Plates were read on a Spectramax M5 microplate reader, with data expressed as the ratio of 665 nm/620 nm fluorescence.

**Scintillation Proximity Binding Assay.** QBI-HEK 293A cells expressing hTP or mTP receptor were grown as described above and harvested in phosphate-buffered saline with 1 mM EDTA. The cell pellet underwent homogenization in 20 mM Hepes, 1 mM EGTA, and 0.5 mM DTT with protease inhibitor cocktail, followed by centrifugation at 1000g for 10 min at 8 °C to remove cell debris. The resulting supernatant was centrifuged at 21 000 rpm for 30 min at 4 °C, with the pellet resuspended in 20 mM Hepes, 1 mM EGTA, 100 mM NaCl. Membrane preparations were normalized to protein level as determined with a bicinchoninic acid assay and stored at –80 °C. Test antagonists were incubated at 10 different concentrations with 100  $\mu\text{g}$  of PVT-WGA SPA beads (PerkinElmer, Waltham, MA, U.S.), 62.5  $\mu\text{g}$  of membrane, and 20 nM <sup>3</sup>H-SQ29,548 (PerkinElmer, Waltham, MA, U.S.) in 50 mM Tris, 4 mM CaCl<sub>2</sub>, 0.1% ascorbic acid, pH 7.5, for 2 h at 25 °C in 384-well polystyrene plates. Plates were sealed and read on a scintillation counter. The percent total binding was determined, with total binding calculated from a minimum of three wells containing membrane, beads, and <sup>3</sup>H-SQ29,548 without antagonist. Nonspecific binding was determined by incubating <sup>3</sup>H-SQ29,548 at multiple concentrations in the presence of 100  $\mu\text{M}$  cold SQ29,548. Binding constants were determined from the determined IC<sub>50</sub> values that were used in the Cheng–Prusoff equation.<sup>23</sup>

## ■ ASSOCIATED CONTENT

**S Supporting Information.** Experimental procedures for the synthesis of compounds **12**, **17–19**, **60–62**; X-ray crystal structures of **7–9** and 2-(cyclopropylmethyl)-3-hydroxycyclopent-2-enone; <sup>1</sup>H NMR spectra of the complex **1**–benzamidine used for Job plot analysis; determination of solubility in acetonitrile for compounds **7–11**; details of computational studies;

analytical reports for pK<sub>a</sub> determinations for compounds **1** and **2**; and pK<sub>a</sub>/log *P* determinations for compounds **7–9**. This material is available free of charge via the Internet at <http://pubs.acs.org>.

## ■ AUTHOR INFORMATION

### Corresponding Author

\*Phone: (215) 898-4891. E-mail: [bcarlo@sas.upenn.edu](mailto:bcarlo@sas.upenn.edu). Address: Department of Chemistry, School of Arts and Sciences, University of Pennsylvania, 231 South 34th Street, Philadelphia, PA 19104-6323.

## ■ ACKNOWLEDGMENT

A.B.S. dedicates this article to William C. Agosta (Professor Emeritus, Rockefeller University, New York, NY), outstanding scientist/scholar, author, and mentor, who first brought to our attention the remarkable acidity of the cyclopentane-1,3-dione class of molecules. Financial support for this work has been provided by the NIH/NIA (Grant AG034140) and the NSF (Grant CHE-0840438, X-ray facility).

## ■ ABBREVIATIONS USED

CPD, cyclopentane-1,3-dione; TP, thromboxane A<sub>2</sub> prostanoid; IP<sub>1</sub>, inositol monophosphate

## ■ REFERENCES

- (1) Patani, G. A.; LaVoie, E. J. Bioisosterism: a rational approach in drug design. *Chem. Rev.* **1996**, *96*, 3147–3176.
- (2) Meanwell, N. A. Synopsis of some recent tactical application of bioisosteres in drug design. *J. Med. Chem.* **2011**, *54*, 2529–2591.
- (3) Herr, R. J. 5-Substituted-1H-tetrazoles as carboxylic acid isosteres: medicinal chemistry and synthetic methods. *Bioorg. Med. Chem.* **2002**, *10*, 3379–3393.
- (4) Boothe, J.; Wilkinson, R.; Kushner, S.; Williams, J. Synthesis of aureomycin degradation products. II. *J. Am. Chem. Soc.* **1953**, *75*, 1732–1733.
- (5) Hiraga, K. Structures of cyclopentanepolyones. *Chem. Pharm. Bull. (Tokyo)* **1965**, *13*, 1300.
- (6) Katrusiak, A. Structure of 1, 3-cyclopentanedione. *Acta Crystallogr., C* **1990**, *46*, 1289–1293.
- (7) Katrusiak, A. Structure of 2-methyl-1, 3-cyclopentanedione. *Acta Crystallogr., C* **1989**, *45*, 1897–1899.
- (8) Dickinson, R. P.; Dack, K. N.; Long, C. J.; Steele, J. Thromboxane modulating agents. 3. 1H-Imidazol-1-ylalkyl- and 3-pyridinylalkyl-substituted 3-[2-[(arylsulfonyl)amino]ethyl]benzenepropanoic acid derivatives as dual thromboxane synthase inhibitor/thromboxane receptor antagonists. *J. Med. Chem.* **1997**, *40*, 3442–3452.
- (9) Koreeda, M.; Liang, Y.; Akagi, H. Easy generation of the dianions of 3-isobutoxycyclopent-2-en-1-ones and their reactions. *J. Chem. Soc., Chem. Commun.* **1979**, 449–450.
- (10) Ramachary, D. B.; Kishor, M. Direct amino acid-catalyzed cascade biomimetic reductive alkylations: application to the asymmetric synthesis of Hajos–Parrish ketone analogues. *Org. Biomol. Chem.* **2008**, *6*, 4176–4187.
- (11) Tilley, J. W.; Danho, W.; Lovey, K.; Wagner, R.; Swistok, J.; Makofske, R.; Michalewsky, J.; Triscari, J.; Nelson, D.; Weatherford, S. Carboxylic acids and tetrazoles as isosteric replacements for sulfate in cholecystokinin analogs. *J. Med. Chem.* **1991**, *34*, 1125–1136.
- (12) Henry, J. R.; Marcin, L. R.; McIntosh, M. C.; Scola, P. M.; Davis Harris, G.; Weinreb, S. M. Mitsunobu reactions of *N*-alkyl and *N*-acyl sulfonamides—an efficient route to protected amines. *Tetrahedron Lett.* **1989**, *30*, 5709–5712.
- (13) Peters, L.; Frohlich, R.; Boyd, A. S. F.; Kraft, A. Noncovalent interactions between tetrazole and an *N,N'*-diethyl-substituted benzamidine. *J. Org. Chem.* **2001**, *66*, 3291–3298.

(14) Tominey, A. F.; Docherty, P. H.; Rosair, G. M.; Quenardelle, R.; Kraft, A. Unusually weak binding interactions in tetrazole–amidine complexes. *Org. Lett.* **2006**, *8*, 1279–1282.

(15) Job, P. Formation and stability of inorganic complexes in solution. *Ann. Chim.* **1925**, *9*, 113–125.

(16) Shenker, A.; Goldsmith, P.; Unson, C. G.; Spiegel, A. M. The G protein coupled to the thromboxane A<sub>2</sub> receptor in human platelets is a member of the novel G<sub>q</sub> family. *J. Biol. Chem.* **1991**, *266*, 9309–9313.

(17) Bylund, D.; Toews, M. Radioligand binding methods for membrane preparations and intact cells. *Methods Mol. Biol. (Clifton, NJ)* **2011**, *746*, 135.

(18) Ruan, K. H.; Wu, J.; So, S. P.; Jenkins, L. A.; Ruan, C. H. NMR structure of the thromboxane A<sub>2</sub> receptor ligand recognition pocket. *Eur. J. Biochem.* **2004**, *271*, 3006–3016.

(19) Hirata, M.; Hayashi, Y.; Ushikubi, F.; Yokota, Y.; Kageyama, R.; Nakanishi, S.; Narumiya, S. Cloning and expression of cDNA for a human thromboxane A<sub>2</sub> receptor. *Nature* **1991**, *349*, 617–620.

(20) Yamamoto, Y.; Kamiya, K.; Terao, S. Modeling of human thromboxane A<sub>2</sub> receptor and analysis of the receptor–ligand interaction. *J. Med. Chem.* **1993**, *36*, 820–825.

(21) Dogne, J.; Hanson, J.; Leval, X.; Pratico, D.; Pace-Asciak, C.; Drion, P.; Pirotte, B.; Ruan, K. From the design to the clinical application of thromboxane modulators. *Curr. Pharm. Des.* **2006**, *12*, 903–923.

(22) Shineman, D. W.; Zhang, B.; Leight, S. N.; Pratico, D.; Lee, V. M. Y. Thromboxane receptor activation mediates isoprostane-induced increases in amyloid pathology in Tg2576 mice. *J. Neurosci.* **2008**, *28*, 4785–4794.

(23) Yung-Chi, C.; Prusoff, W. H. Relationship between the inhibition constant (K<sub>i</sub>) and the concentration of inhibitor which causes 50 per cent inhibition (I<sub>50</sub>) of an enzymatic reaction. *Biochem. Pharmacol.* **1973**, *22*, 3099–3108.